

Vestiges of Topological Phase Transitions in Kitaev Quantum Spin Liquids

Ara Go,^{1,*} Jun Jung,^{2,*} and Eun-Gook Moon^{2,†}

¹*Center for Theoretical Physics of Complex Systems,
Institute for Basic Science (IBS), Daejeon 34126, Korea*

²*Department of Physics, KAIST, Daejeon 34141, Korea*

(Dated: December 15, 2024)

We investigate signatures of topological quantum phase transitions (TQPTs) between the Z_2 quantum spin liquids (QSLs). In two spatial dimensions, Z_2 QSLs and their TQPTs are only well-defined at zero temperature ($T = 0$), and it is imperative to clarify their non-zero temperature observable signatures. Here, we present the vestiges of TQPTs between Z_2 QSLs with Majorana fermions in terms of thermal Hall conductivity κ_{xy} at non-zero temperatures. The κ_{xy}/T shows characteristic temperature dependences around TQPTs. We argue that an exponential upturn near $T = 0$ and the peak of κ_{xy}/T around massive excitation energy are observable smoking-gun signals of the TQPTs. Quantum critical fan-shape temperature dependences are uncovered across TQPTs. We also perform the parton mean-field analysis on a modified Kitaev model with next-nearest neighbor interactions finding TQPTs between the phases with different Chern numbers and their vestiges self-consistently. We discuss the implication of our results to the recent experiments in $\alpha\text{-RuCl}_3$.

Introduction : Quantum spin liquids intrinsically host enormous entanglements, manifested by emergent excitations, fractionalized particles and gauge fluctuations [1, 2]. Theoretical investigations, mostly using parton constructions [3, 4], deepen our understanding in characteristics of QSLs, and even the existence of Z_2 QSLs of spin 1/2 systems on a honeycomb lattice is shown by an exactly solvable model, so-called Kitaev model [5]. The Kitaev representation of spins, $\vec{S} = i\vec{c}\vec{b}$ with four majorana fermions (c, \vec{b}), is used to prove the existence of a topological phase with the Chern number $|\nu| = 1$. In this work, Z_2 QSLs with Majorana fermions as elementary excitations are called Kitaev QSLs.

Important advances in Kitaev QSLs were achieved by Jackeli and Khaliullin who showed strongly spin-orbit coupled honeycomb lattices may host the Kitaev model in 2D [6]. Several materials with 4d and 5d orbital degrees of freedom including $\alpha\text{-RuCl}_3$ have been suggested as candidates [7–10]. Extensive experimental works have been reported in neutron, specific heat, nuclear magnetic resonance, magnetic torque, and thermal conductivity in the materials [11–20]. Especially, the recent thermal conductivity experiment on $\alpha\text{-RuCl}_3$ reported the quantized thermal Hall conductivity of $\kappa_{xy}/T = (\pi/12)(k_B^2/\hbar)$ below 5K, a hall-mark of a Majorana edge mode [20]. In the experiment, a peak was observed around 10K, where gauge flux gap was found [15]. Its origin remains as an intriguing open question.

Topological properties of Kitaev QSLs are not well-defined at non-zero temperatures and adiabatically connected to high temperature paramagnetic states. Since it is impossible to detect topological properties sharply at

non-zero temperatures, it is quintessential to search for vestiges of topological properties such as the quantization behavior of κ_{xy}/T at sufficiently low temperatures. In this letter, we investigate vestiges of TQPTs in Kitaev QSLs by using path-integral and parton mean-field analysis. It is shown that characteristic temperature dependence of κ_{xy}/T may appear around TQPTs, and we propose them as smoking-gun signatures of TQPTs.

Path-integral formalism: The Kitaev representation gives a Hilbert space of Majorana fermions, whose dimension is larger than one of spins. To describe spin physics, it is crucial to project out unphysical states in the Majorana Hilbert space. One conventional way is to define the projection operator, $\mathcal{P} = \prod_j (\frac{1+b_j^x b_j^y b_j^z c_j}{2})$ with a site index j [5], and a spin state is obtained by applying the operator to a Majorana state, $|\Psi_{\text{spin}}\rangle = \mathcal{P}|\Psi_{\text{Majorana}}\rangle$. However, it may be subtle and difficult to employ the projection operator for calculations of physical quantities such as dynamic spin susceptibility [21]. A priori, one should first check whether a Majorana state, which may be obtained by the parton mean field analysis, produces a well-defined spin state. Below, we consider the path-integral formalism and find non-perturbative properties which allow us to circumvent a part of the subtleties and difficulties from the projection operator.

We use the path-integral formalism with four Majorana fermions, and the partition function is

$$\mathcal{Z} = \int \mathcal{D}c \mathcal{D}\vec{b} \prod \delta(b^x b^y b^z c - 1) e^{-S}.$$

Remark that the product of the delta functions precisely describes the projection operator with the implicit space-time index. The action of the spin Hamiltonian

* The first two authors contribute equally to this work.

† egmoon@kaist.ac.kr

$H_{\text{spin}}(\{\vec{S}_j\})$ is

$$\mathcal{S} = \int_0^\beta d\tau \sum_j (c_j \partial_\tau c_j + \vec{b}_j \partial_\tau \vec{b}_j) + \int_0^\beta d\tau H_{\text{spin}}(\{c\}, \{\vec{b}\}).$$

For a generic spin Hamiltonian, $H_{\text{spin}} = \sum_{j,k,\alpha,\beta} J_{jk}^{\alpha\beta} S_j^\alpha S_k^\beta$, we introduce three Hubbard-Stratonovich (HS) fields $(\lambda_j, u_{jk}, v_{jk})$, which give $\mathcal{Z} = \int \mathcal{D}c_j \mathcal{D}\vec{b}_j \mathcal{D}\lambda_j \mathcal{D}u_{ij} \mathcal{D}v_{ij} e^{-\mathcal{S}_{\text{eff}}}$. The effective action is

$$\begin{aligned} \mathcal{S}_{\text{eff}} = & \int_0^\beta d\tau \sum_j c_j \partial_\tau c_j + \vec{b}_j \partial_\tau \vec{b}_j + \lambda_j (b_j^x b_j^y b_j^z c_j - 1) \\ & + \int_0^\beta d\tau \sum_{j,k} (-i) u_{jk} c_j c_k + (+i) v_{jk} J_{jk}^{\alpha\beta} b_j^\alpha b_k^\beta - u_{jk} v_{jk}. \end{aligned}$$

The Lagrange multiplier field λ is redefined to absorb the factor i as usual. One advantage of the path-integral formalism is that the projection operator can be treated as the four-fermion interaction term with λ . We emphasize that no approximation is made in \mathcal{Z} and the projection/interaction terms are simply rewritten in terms of the HS fields $(u_{jk}, v_{jk}, \lambda_j)$, which allows non-perturbative analysis below.

First, a quantum state without mixing c and \vec{b} Majorana fermions ($|\Psi_M\rangle \equiv |\{c\}\rangle \otimes |\{\vec{b}\}\rangle$) describes a paramagnetic state because of the properties, $\langle\{c\}|c_j|\{c\}\rangle = \langle\{\vec{b}\}|\vec{b}_j|\{\vec{b}\}\rangle = 0$, which is our main focus in this work. The projection operator is spin-singlet, so the corresponding spin state describes a QSL. In the path-integral formalism, the non-mixing condition indicates that the four-fermion interaction term $(b_j^x b_j^y b_j^z c_j)$ is sub-dominant. If the interaction term is rewritten with an additional HS field, its mean value is zero for a QSL because of $\vec{S} = i\epsilon\vec{b}$.

Second, for a gapped QSL, the standard stationary approximation to the partition function is safe. Namely, a self-consistent mean-field solution is reliable, and the HS fields may be replaced by their mean-values, $\bar{u}_{jk} \equiv (+i)\langle J_{jk}^{\alpha\beta} b_j^\alpha b_k^\beta \rangle$, $\bar{v}_{jk} = (-i)\langle c_j c_k \rangle$ omitting the bar notations hereafter. The four Majorana bands are well-defined with the Chern numbers (ν_n) and bulk energy gaps (Δ_n) with a band index, $n = 1, 2, 3, 4$. The total Chern number is $\nu \equiv \sum_n (\bar{\nu}_n) = \sum_n \nu_n$, and stability of a gapped QSL is guaranteed by the energy gaps. At a TQPT, an energy gap closes (say, $\Delta_4 = 0$), and if it closes only at few points in Brillouin zone with linear dispersion relations, the projection/interaction terms are irrelevant as in the B phase of the Kitaev model [5]. We consider such TQPTs in this work. The path-integral formalism demonstrates the existence of the gapped QSLs and their TQPTs with mean-field ansatzes. It also shows that the phases and their transitions are not destabilized by the four-point interaction term from the projection operator.

Armed with the non-perturbative properties, an edge theory of a gapped Kitaev QSL is naturally constructed, $\mathcal{L}_{\text{edge}} = \psi_n \partial_\tau \psi_n + \psi_n \epsilon_n (-i \partial_x) \psi_n$, with an edge coor-

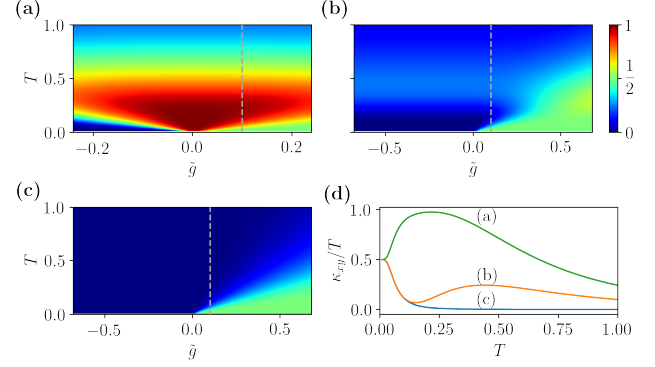


FIG. 1. $\kappa_{xy}^{\text{edge}}/T$ near TQPTs between the phases with $\nu = 0$ and $\nu = 1$. The units of $\kappa_{xy}^{\text{edge}}/T$ and T are $(\pi/6)(k_B^2/\hbar^2)$ and $\Delta_1/2$, respectively. The smallest gap depends on $|\tilde{g}|$ linearly, ($\Delta_4 = \Delta_1|\tilde{g}|$). $\tilde{g} > \tilde{g}_c$ is for the phases with $\nu = 1$, and its false color representations of $\kappa_{xy}^{\text{edge}}/T$ are given in (a)-(c). TQPT between (a) $\tilde{\nu} = (1, 1, 0, -2)$ and $(1, 1, 0, -1)$ with $\Delta_1 = 2$ and $\Delta_2 = 1$, (b) $\tilde{\nu} = (1, -1, 0, 0)$ and $(1, -1, 0, 1)$ with $\Delta_1 = 2$ and $\Delta_2 = 1$, and (c) $\tilde{\nu} = (1, -1, 0, 0)$ and $(1, -1, 0, 1)$ with $\Delta_1 = \Delta_2 = 2$. (d) $\kappa_{xy}^{\text{edge}}/T$ at $\tilde{g} = 0.1$ (marked by dashed lines in (a)-(c)).

dinate (x), energy dispersion $\epsilon_n(k_x)$, and real Grassmann field ψ_n . The energy dispersion of a chiral mode is well-defined in the interval $\epsilon_n(k_x) \in (0, \Delta_n)$ if $\nu_n \neq 0$. Defining an edge thermal current, $J_e(T) = \sum_n \int \frac{dk_x}{2\pi} v_n(k_x) \epsilon_n(k_x) f(\epsilon_n(k_x))$ with a velocity of the mode (v_n) and the Fermi distribution function (f), the thermal Hall conductivity divided by temperature is obtained,

$$\frac{\kappa_{xy}^{\text{edge}}}{T} = \sum_n \nu_n \left(\frac{\pi}{12} - \frac{1}{2\pi T^3} \int_{\Delta_n}^{\infty} \frac{\epsilon^2 e^{\epsilon/T}}{(1 + e^{\epsilon/T})^2} d\epsilon \right). \quad (1)$$

We use the units ($k_B = \hbar = 1$) (see SI for detailed information on its derivation). The edge current becomes precise when bulk bands are flat (localized). Its quantization is obvious in the zero temperature limit ($\kappa_{xy}^{\text{edge}}/T \rightarrow \nu\pi/12$).

Near a TQPT, we introduce a parameter \tilde{g} to describe a gapped Kitaev QSL with ν ($\tilde{g} < \tilde{g}_c$) and the one with $\nu + 1$ ($\tilde{g} > \tilde{g}_c$). A critical value \tilde{g}_c is set to be zero hereafter. We assume the lowest energy gap has the dependence $\Delta_4 \propto |\tilde{g}|$ near the TQPT and the corresponding mode has a linear dispersion relation, which is supported by our parton mean-field analysis below. Generalization to generic TQPTs is straightforward. At the quantum critical point, using the edge theory Eqn.(1) may be subtle, but as shown below, the edge theory results are well matched with the bulk theory calculations. Ignoring \tilde{g} dependences of the bigger energy gaps ($\Delta_{1,2,3}$), we illustrate $\kappa_{xy}^{\text{edge}}/T$ for TQPTs between $\nu = 0$ and $\nu = 1$ in Fig. 1. Striking temperature dependences appear at non-zero temperatures, characterized by the structures of (ν_n, Δ_n) , as shown in Fig 1(a)-(c). Detailed conditions of (ν_n, Δ_n) are explained in the caption.

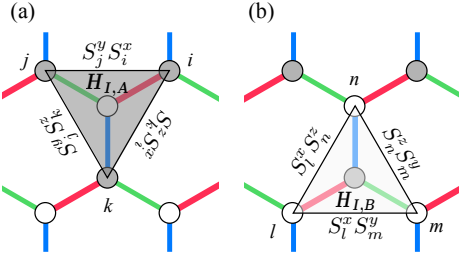


FIG. 2. Graphical representation of the NNN spin exchange interactions of sublattice (a) A and (b) B . Sites of different sub-lattices are illustrated by white and gray circles. The nearest neighbor bonds which correspond to $S^x S^x$, $S^y S^y$ and $S^z S^z$ in the Kitaev Hamiltonian are plotted by red, green, and blue lines respectively.

The critical-fan shapes manifest around $(\tilde{g}_c = 0, T = 0)$ in Fig. 1(a), and the fan-shapes appear in $\tilde{g}_c > 0$ in Fig. 1(b) and (c). We present the characteristic curves for the $\nu = 1$ phases (along the $\tilde{g} = 0.1$ line in (a)-(c)) in Fig. 1(d). At $\tilde{g} = 0.1$ in (a), we find

$$\frac{\kappa_{xy}^{\text{edge}}}{T} \simeq \frac{\pi}{12} + \alpha_1 \left(\frac{\Delta_4}{T} \right)^2 e^{-\frac{\Delta_4}{T}}, \quad \alpha_1 > 0, \quad (2)$$

in the limit of $T \ll \Delta_4$ with the conditions $\Delta_1 = 2\Delta_2 \gg \Delta_4$ and $\vec{\nu} = (1, 1, -1, 0)$.

The temperature dependence of the upturn is exponential, and the peak of κ_{xy}/T appears around $T \sim \Delta_4$ where its height depends on $\nu_{1,2,3}$ and $\Delta_{1,2,3}$. We propose the existence of the peak with the exponential upturn as a smoking-gun signature of a TQPT between $\nu = 0$ and $\nu = 1$. On the other hand, the cases (b) and (c) show $\kappa_{xy}^{\text{edge}}/T = \pi/12 - \alpha_2(\Delta_4/T)^2 e^{-\Delta_4/T}$, with a positive constant α_2 . Such temperature dependences are similar to the ones of the original Kitaev model under weak magnetic field [22] but are significantly different from the ones in experiments [20].

The qualitative differences between (a), (b), and (c) are originated from the overall structure of (Δ_n, ν_n) . Though the total Chern number is only important near $T = 0$, all the Chern numbers and band gaps become relevant at non-zero temperatures. Thus, not only the matter Majorana fermions (c) but also the gauge-flux Majorana fermions (\vec{b}) can contribute to thermal Hall conductivity and it is crucial to keep both of them at non-zero temperatures.

Parton mean-field analysis: To understand TQPTs with a microscopic perspective, let us consider a modified Kitaev Hamiltonian, $H_{\text{tot}} = H_K + g(H_{I,A} + H_{I,B})$, with a dimensionless parameter (g). We find that the

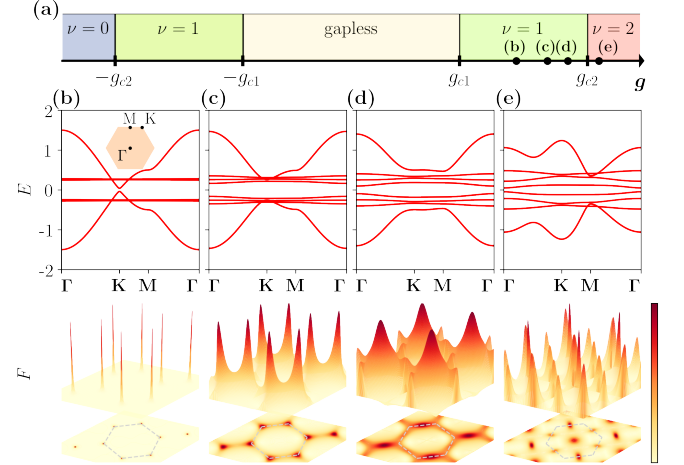


FIG. 3. (a) Phase diagram of $H_{\text{tot}} = H_K + g(H_{I,A} + H_{I,B})$ with parton mean-field analysis. Band structure along the high symmetry line for few selected values of g , (b) $g=1.6$, (c) $g=1.9$, (d) $g=2.1$, and (e) $g=2.3$. The corresponding Berry curvature in the momentum space are given below the band structure. The first Brillouin zone is marked by dashed lines in the projection.

next-nearest neighbor (NNN) interaction terms,

$$H_{I,A} = -\frac{K}{2} \sum_{\nabla,ijk} S_i^x S_j^y + S_j^y S_k^z + S_k^z S_i^x$$

$$H_{I,B} = -\frac{K}{2} \sum_{\triangle,lmn} S_l^x S_m^y + S_m^y S_n^z + S_n^z S_l^x,$$

captures TQPTs nicely. The summations over ∇, \triangle are graphically represented in Fig. 2. The original Kitaev Hamiltonian $H_K = -K \sum_{\langle i,j \rangle} S_j^{\alpha_{jk}} S_k^{\alpha_{jk}}$ is used whose link dependent exchange interactions with α_{jk} are given in [5]. For simplicity, we consider the isotropic exchange interactions, and its generalization to anisotropic cases is straightforward.

For $g = 0$, the ansatz, $u_0 = \langle i c_j c_k \rangle$ and $u = \langle i b_j^{\alpha_{jk}} b_k^{\alpha_{jk}} \rangle$ with the nearest neighbor indices (j, k) is used, and the mean-field Hamiltonian is

$$H_K^{\text{MF}} = -K \sum_{\langle j,k \rangle} [u (i c_j c_k) + u_0 (i b_j^{\alpha_{jk}} b_k^{\alpha_{jk}}) - u_0 u].$$

We find ($u_0 = -0.5249$, $u = +1$) giving the gapless excitations of c Majorana fermions and the flat bands of \vec{b} Majorana fermions, which are precisely the same as the previous literature [23].

For $g \neq 0$, we extend our mean-field analysis by introducing mean-values for the NNN interaction terms, $w_0 = \langle i c_j c_k \rangle$ and $w = \langle i b_l^x b_m^y \rangle$ with the NNN indices

(j, k, l, m) . The mean-field ansatz gives

$$\begin{aligned} H_{I,A}^{\text{MF}} &= \frac{K}{2} \sum_{\nabla,ijk} w \left(i c_{A,i} c_{A,j} \right) - w_0 \left(i b_{A,i}^x b_{A,j}^y \right) \\ &\quad + w_0 w + ((x, y, z) \text{ cyclic terms}), \\ H_{I,B}^{\text{MF}} &= \frac{K}{2} \sum_{\Delta,lmn} w \left(i c_{B,l} c_{B,m} \right) - w_0 \left(i b_{B,l}^x b_{B,m}^y \right) \\ &\quad + w_0 w + ((x, y, z) \text{ cyclic terms}), \end{aligned}$$

where the sublattice index (A, B) is shown explicitly for clarity. The summation over the triangle and reverse-triangle are done in the clock and counter-clock wise directions. Non-zero values of w, w_0 breaks time-reversal symmetry, and their form is equivalent to the effects of a weak external magnetic field along the $(1, 1, 1)$ direction in perturbative analysis [5]. In this sense, our parton mean-field analysis captures physics of the original Kitaev model under an external magnetic field by using spontaneous symmetry breaking. For simplicity, we keep a three-fold rotational symmetry, but weak symmetry breaking effects do not change our conclusions since topological phases are gapped.

We find three different phases separated by $g_{c1} \sim 1.05$ and $g_{c2} \sim 2.25$ for $g > 0$. For $g < 0$, only the Chern numbers of \vec{b} Majorana fermions are opposite to the ones at $|g|$.

1) $g < g_{c1}$, the ansatz and the band structures are the same as the ones of $g = 0$. Time reversal symmetry is not broken.

2) $g_{c1} < g < g_{c2}$, all the mean-values are non-zero breaking time reversal symmetry. The typical band structures and corresponding Berry curvature $F(\mathbf{k})$ are illustrated in Fig. 2. Clearly, all the bands are gapped and dispersive. We find the Chern numbers of \vec{b} Majorana fermions $(-1, 0, 1)$ respectively.

3) $g_{c2} < g$, we find a topological phase with $\nu = 2$. At $g = g_{c2}$, one of the \vec{b} Majorana bands become gapless while the c Majorana fermions remain gapped, and the gapless excitation appears at Γ with a linear dispersion relation. Our results self-consistently show the two different channels of TQPTs as in the previous analysis with vortex lattices [24].

The bulk thermal Hall conductivity is computed by using the conventional formula [25, 26]

$$\frac{\kappa_{xy}^{\text{bulk}}}{T} = -\frac{1}{T^2} \int d\epsilon \epsilon^2 \frac{\partial f(\epsilon, T)}{\partial \epsilon} \sum_{\mathbf{k}, \varepsilon_n(\mathbf{k}) < \epsilon} F_n(\mathbf{k}), \quad (3)$$

where the \mathbf{k} summation runs over the first Brillouin zone and $\varepsilon_n(\mathbf{k})$ is the n th energy eigenvalue of the mean-field Hamiltonian. At $T \rightarrow 0$, $\kappa_{xy}^{\text{bulk}}/T$ is quantized as $\nu\pi/12$ same as Eq. (1).

In Fig. 4(a), the density plot of $\kappa_{xy}^{\text{bulk}}/T$ is illustrated. Qualitative dependences on T and g are similar to Fig. 1. For example, the critical-fan shape appears as in Fig. 1(b)

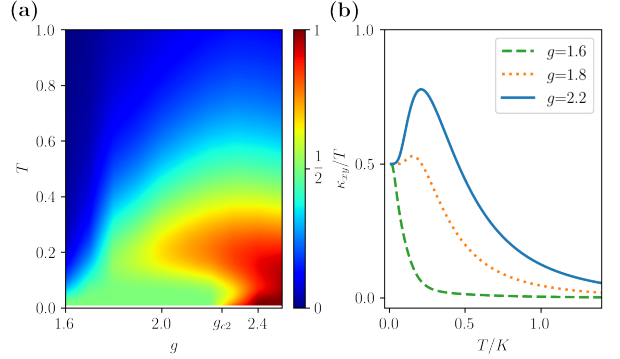


FIG. 4. (a) False color representation of κ_{xy}/T on $g - T$ plane with $g_{c2} \sim 2.25$. (b) T -dependence of κ_{xy}/T for $g = 1.6$ (dashed), 1.8 (dotted), 2.2 (plain). The unit of κ_{xy}/T is the same as in Fig. 1.

and (c) near g_{c2} , but away from g_{c2} , it is more distorted than Fig. 1 because higher energy bands depend on g and have dispersive spectrums. In Fig. 4(b), temperature dependences of $\kappa_{xy}^{\text{bulk}}/T$ for different values of g are illustrated. For $g = 1.6$, $\kappa_{xy}^{\text{bulk}}/T$ shows monotonic temperature dependence, but for $g = 2.2$, non-monotonic temperature dependences appear with a peak around $T/K \sim \Delta_4$ and, for $T \ll \Delta_4$, the upturn temperature dependence is exponential. The bigger band gaps $\Delta_{1,2}$ is an order of magnitude larger than Δ_4 , and the Chern number vector is $\vec{\nu} = (1, 1, 0, -1)$. The qualitative matching between $\kappa_{xy}^{\text{edge}}/T$ and $\kappa_{xy}^{\text{bulk}}/T$ is one sanity check of our analysis.

Discussion and conclusion: Our calculations of κ_{xy}/T illustrate vestiges of TQPTs at non-zero temperatures. We note that in experiments κ_{xy}/T includes phonon contributions, but recent theoretical works reported that the phonon contributions to κ_{xy}/T may be negligible to the quantized value [27, 28]. Furthermore, the phonon contributions are estimated to show power-law temperature dependent corrections, $\kappa_{xy,\text{phonon}}/T \sim T^2$, to the quantized values, which was applied to the upturn of κ_{xy}/T in $\alpha\text{-RuCl}_3$ [28]. We, instead, propose the vestiges of a TQPT as an alternative route presenting the exponential upturn and the peak around massive excitation energy as shown in Fig. 1 and 4. Further detailed measurements of temperature dependence of $\kappa_{xy}(T)/T$ may distinguish the two scenarios.

We stress that all Majorana fermions (c, \vec{b}) may contribute to physical quantities near generic TQPTs. This is in drastic contrast to the original Kitaev model with weak perturbations where only c Majorana fermions are important at low temperatures. Our calculations with the edge and the parton mean-field theories naturally capture the contributions of all the Majorana fermions, and $\kappa_{xy}^{\text{edge}}/T$ is *asymptotically exact* at low temperatures. The exponential upturn followed by the peak of κ_{xy}/T is a concrete prediction of our results, which makes quantum critical-fan shape dependence around TQPTs reliable. At topological quantum critical points, additional

scattering mechanisms between gapless modes could appear which might be important. Future works which consider the scattering mechanisms near TQPTs with acoustic phonons are desirable.

In this work, we use κ_{xy}/T for vestiges of TQPTs since it is directly related to the Chern number in $T \rightarrow 0$, but other physical quantities such as specific heat, nuclear magnetic resonances, and neutron experiments would also show signatures of TQPTs. Further research on the physical quantities with a perspective of TQPTs would be highly desired. Also, numerical and theoretical works on realistic magnetic Hamiltonians including Heisenberg, Γ interactions, and magnetic fields would be important [29–31]. We emphasize that our analysis can be readily extended beyond the scope of the Kitaev QSLs. The phenomenological nature with (Δ_n, ν_n) should be applicable to generic Z_2 QSLs as well as conventional phases with topologically non-trivial structures, for example spin-

wave bands [32, 33].

In conclusion, we study the vestiges of TQPTs in Kitaev QSLs by using path-integral and parton mean-field analysis. Around TQPTs, characteristic temperature dependences of κ_{xy}/T are obtained, including quantum-critical fan-shape dependences, and we provide smoking-gun signatures of TQPTs which may be tested in future experiments.

Acknowledgement: We thank E. Berg, L. Janssen, Y. B. Kim, Y. Matsuda, Y. Motome, N. Perkins, and A. Rosch for invaluable discussions and comments. EGM is grateful to A. Furusaki, Y. Mastuda and Y. Motome for their hospitalities during the visits to RIKEN, Kyoto University, and University of Tokyo. This work was supported by NRF of Korea under Grant No. 2017R1C1B2009176 (JJ, EGM), and Institute for Basic Science (IBS) in Korea under Grant No. IBS-R024-D1 (AG).

-
- [1] Y. Zhou, K. Kanoda, and T.-K. Ng, Rev. Mod. Phys. **89**, 025003 (2017).
- [2] L. Savary and L. Balents, Rep. Prog. Phys. **80**, 016502 (2017).
- [3] S. Sachdev, *Quantum phase transitions*, 2nd ed. (Cambridge University Press, Cambridge, 2011).
- [4] X. G. Wen, *Quantum Field Theory of Many-Body Systems* (Oxford University Press, Oxford, 2004).
- [5] A. Kitaev, Annals of Physics **321**, 2 (2006).
- [6] G. Jackeli and G. Khaliullin, Phys. Rev. Lett. **102**, 017205 (2009).
- [7] J. Nasu, M. Udagawa, and Y. Motome, Phys. Rev. Lett. **113**, 197205 (2014).
- [8] I. Rousochatzakis, J. Reuther, R. Thomale, S. Rachel, and N. B. Perkins, Phys. Rev. X **5**, 041035 (2015).
- [9] S. Trebst, arXiv:1701.07056.
- [10] H.-S. Kim, V. Shankar V., A. Catuneanu, and H.-Y. Kee, Phys. Rev. B **91**, 241110 (2015).
- [11] A. Banerjee, C. A. Bridges, J. Q. Yan, A. A. Aczel, L. Li, M. B. Stone, G. E. Granroth, M. D. Lumsden, Y. Yiu, J. Knolle, S. Bhattacharjee, D. L. Kovrizhin, R. Moessner, D. A. Tennant, D. G. Mandrus, and S. E. Nagler, Nature Materials **15**, 733 (2016).
- [12] S.-H. Do, S.-Y. Park, J. Yoshitake, J. Nasu, Y. Motome, Y. S. Kwon, D. T. Adroja, D. J. Voneshen, K. Kim, T. H. Jang, J. H. Park, K.-Y. Choi, and S. Ji, Nature Physics **13**, 1079 (2017).
- [13] L. J. Sandilands, Y. Tian, K. W. Plumb, Y.-J. Kim, and K. S. Burch, Phys. Rev. Lett. **114**, 147201 (2015).
- [14] J. Nasu, J. Knolle, D. L. Kovrizhin, Y. Motome, and R. Moessner, Nature Physics **12**, 912 (2016).
- [15] S.-H. Baek, S.-H. Do, K.-Y. Choi, Y. S. Kwon, A. U. B. Wolter, S. Nishimoto, J. van den Brink, and B. Büchner, Phys. Rev. Lett. **119**, 037201 (2017).
- [16] A. U. B. Wolter, L. T. Corredor, L. Janssen, K. Nenkov, S. Schönecker, S.-H. Do, K.-Y. Choi, R. Albrecht, J. Hunger, T. Doert, M. Vojta, and B. Büchner, Phys. Rev. B **96**, 041405 (2017).
- [17] I. A. Leahy, C. A. Pocs, P. E. Siegfried, D. Graf, S.-H. Do, K.-Y. Choi, B. Normand, and M. Lee, Phys. Rev. Lett. **118**, 187203 (2017).
- [18] Y. Kasahara, K. Sugii, T. Ohnishi, M. Shimozawa, M. Yamashita, N. Kurita, H. Tanaka, J. Nasu, Y. Motome, T. Shibauchi, and Y. Matsuda, Phys. Rev. Lett. **120**, 217205 (2018).
- [19] N. Janša, A. Zorko, M. Gomilšek, M. Pregelj, K. W. Krämer, D. Biner, A. Biffin, C. Rüegg, and M. Klanjšek, Nature Physics (2018).
- [20] Y. Kasahara, T. Ohnishi, Y. Mizukami, O. Tanaka, S. Ma, K. Sugii, N. Kurita, H. Tanaka, J. Nasu, Y. Motome, T. Shibauchi, and Y. Matsuda, Nature **559**, 227 (2018).
- [21] J. Knolle, S. Bhattacharjee, and R. Moessner, Phys. Rev. B **97**, 134432 (2018).
- [22] J. Nasu, J. Yoshitake, and Y. Motome, Phys. Rev. Lett. **119**, 127204 (2017).
- [23] Y.-Z. You, I. Kimchi, and A. Vishwanath, Phys. Rev. B **86**, 085145 (2012).
- [24] V. Lahtinen, A. W. W. Ludwig, J. K. Pachos, and S. Trebst, Phys. Rev. B **86**, 075115 (2012).
- [25] O. Vafek, A. Melikyan, and Z. Tešanović, Phys. Rev. B **64**, 224508 (2001).
- [26] H. Sumiyoshi and S. Fujimoto, J. Phys. Soc. Jpn. **82**, 023602 (2013).
- [27] M. Ye, G. B. Halász, L. Savary, and L. Balents, arXiv:1805.10532.
- [28] Y. Vinkler-Aviv and A. Rosch, arXiv:1805.11587.
- [29] A. Catuneanu, Y. Yamaji, G. Wachtel, Y. B. Kim, and H.-Y. Kee, npj Quantum Materials **3**, 23 (2018).
- [30] J. Nasu, Y. Kato, Y. Kamiya, and Y. Motome, arXiv:1805.02423.
- [31] C. Hickey and S. Trebst, arXiv:1805.05953.
- [32] J. Cookmeyer and J. E. Moore, arXiv:1807.03857.
- [33] F. Lu and Y.-M. Lu, arXiv:1807.05232.

Vestiges of Topological Phase Transitions in Kitaev Quantum Spin Liquids: Supplementary Information

I. EDGE THEORY OF THERMAL HALL CONDUCTIVITY

To be self-contained, we present the derivation of κ_{xy}/T by using the edge theory. We follow the notation of Ref. S1. The temperatures along the top and bottom edges, T_{top} and T_{bot} , are constant and the total energy current through the system is given by $J_T = J_e(T_{top}) - J_e(T_{bot})$. For small temperature difference, the thermal current and the thermal Hall conductivity are

$$J_T = \frac{dJ_e(T)}{dT}(T_{top} - T_{bot}), \quad \kappa_{xy} = \frac{dJ_e(T)}{dT}.$$

For a single chiral fermionic channel with arbitrary dispersion ϵ_{k_x} , one finds

$$\frac{dJ_e(T)}{dT} = \int \frac{dk_x}{2\pi} \epsilon_{k_x} v_{k_x} \frac{df(\epsilon_{k_x})}{dT} = - \int_{\epsilon_{min}}^{\epsilon_{max}} \frac{\epsilon^2 f'(\epsilon)}{2\pi T} d\epsilon.$$

with $v_{k_x} = \frac{d\epsilon_{k_x}}{dk_x}$. The chiral edge mode energy cutoffs are $\epsilon_{min} = 0$ and $\epsilon_{max} = \Delta$ where Δ is a bulk energy gap. Thus, we find the formulas,

$$\frac{dJ_e(T)}{dT} = \int_0^\Delta \frac{\epsilon^2}{2\pi T^2} \frac{e^{\epsilon/T}}{(1 + e^{\epsilon/T})^2} d\epsilon \quad (\text{S1})$$

and

$$\frac{\kappa_{xy}}{T} = \frac{\pi}{12} - \int_\Delta^\infty \frac{\epsilon^2}{2\pi T^3} \frac{e^{\epsilon/T}}{(1 + e^{\epsilon/T})^2} d\epsilon \quad (\text{S2})$$

Generalizing it, we obtain the formula,

$$\frac{\kappa_{xy}}{T} = \sum_n \nu_n \left(\frac{\pi}{12} - \frac{1}{2\pi T^3} \int_{\Delta_n}^\infty \frac{\epsilon^2 e^{\epsilon/T}}{(1 + e^{\epsilon/T})^2} d\epsilon \right), \quad (\text{S3})$$

and we illustrate κ_{xy}/T for $\vec{\nu} = (1, 1, 0, -1)$ and $\vec{\Delta} = (2, 1, 1, 0.1)$ with a proper unit in Fig. S1.

II. MEAN-FIELD ORDER PARAMETERS

The order parameters obtained by self-consistent mean-field calculations are given in Fig. S2. As described in the main text, the nearest-neighbor interactions are decoupled by using the order parameters (u_0, u) while the next-nearest-neighbor ones are associated with (w_0, w) . In the gapless phase ($g < g_{c1}$), the original Kitaev solution ($u_0 = 0.5249, u = 1$) [S2] is reproduced. The order parameters (w_0, w) converge to nonzero values where the Chern number is well-defined as $\nu = 1$.

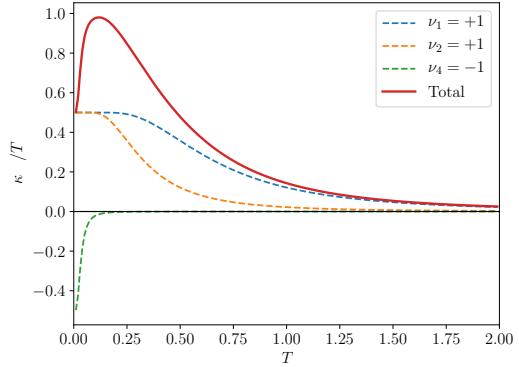


FIG. S1. κ_{xy}/T from Majorana fermions. The red thick line is for the total κ_{xy}/T . The blue (orange) dashed line is for the contribution of $\nu_1 = 1$ ($\nu_2 = 1$) and $\Delta = 2$ ($\Delta = 1$) to κ_{xy}/T . The green dashed line is for the contribution of $\nu_4 = -1$ and $\Delta = 0.1$ to κ_{xy}/T . The different gap energy scales with the Chern numbers determine the peak position and height.

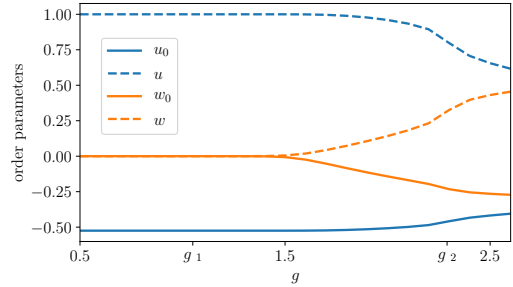


FIG. S2. Mean-field order parameters across the phase transitions at g_{c1} (from gapless to $\nu = 1$) and g_{c2} (from $\nu = 1$ to $\nu = 2$).

III. BERRY CURVATURE AND CHERN NUMBER

The Berry curvature of n th band of the mean-field Hamiltonian at momentum \mathbf{k} is computed from the Bloch function $u_{n\mathbf{k}}$ as Ref. S3

$$F_n(\mathbf{k}) = \frac{\partial}{\partial k_x} A_{k_y}(\mathbf{k}) - \frac{\partial}{\partial k_y} A_{k_x}(\mathbf{k}), \quad (\text{S4})$$

where the Berry connection $A_{k_\alpha} = \langle u_{n\mathbf{k}} | \frac{\partial}{\partial k_\alpha} | u_{n\mathbf{k}} \rangle$ with $\alpha = x, y$. Then the Chern number of the band ν_n is given by integration over the Brillouin zone as

$$\nu_n = \frac{1}{2\pi i} \int_{B.Z} d\mathbf{k} F_n(\mathbf{k}). \quad (\text{S5})$$

IV. APPLICATION TO α -RUCL₃

In this section, we discuss a possible scenario of α -RuCl₃ in terms of a TQPT starting from the original Kitaev model. In experiments, the TQPT is suggested at high magnetic fields based on the change of the Chern numbers from $\nu = 1$ to $\nu = 0$.

We assume the three conditions. First, the phenomenological parameter dependence is $\tilde{g} \propto -B_{\parallel}$ near the TQPT. Second, the band gaps and Chern numbers have the same structures as ones of Fig. 1(a). The Chern number vector changes from $\vec{\nu} = (1, 1, 0, -1)$ to $(1, 1, 0, -2)$, and the smallest gap around the TQPT is associated with the $\nu_4 = -1$ band. Third, the $\nu = 1$

phase ($\tilde{g} > 0$) in Fig. 1(a) is connected to the original Kitaev model with a small magnetic field. The perturbative calculation and parton mean field analysis show that the Chern number vector $\vec{\nu} = (1, 0, -1, 1)$, and the smallest gap is associated with the $\nu_4 = 1$ band.

We propose *a band crossing* to connect the $\nu = 1$ phase in Fig. 1(a) with one of the Kitaev model under a weak magnetic field. The crossing is inevitable because the lowest energy band changes the Chern number from $\nu_4 = 1$ to $\nu_4 = -1$. There are no changes in symmetry and topology, but the band crossing signatures would be observable energetically. Note that, in reality, the magnetically ordered state exists, so one should keep in mind that the band crossing point may be masked by the ordered phase.

[S1] Y. Vinkler-Aviv and A. Rosch, arXiv:1805.11587.

[S2] A. Kitaev, Annals of Physics **321**, 2 (2006).

[S3] D. Xiao, M.-C. Chang, and Q. Niu, Rev. Mod. Phys. **82**, 1959 (2010).